Biochimica et Biophysica Acta 1838 (2014) 932–939

Contents lists available at ScienceDirect

Biochimica et Biophysica Acta

journal homepage: www.elsevier.com/locate/bbamem

Mutations adjacent to the end of transmembrane helices 6 and 7 independently affect drug efflux capacity of yeast ABC transporter Pdr5p

Zhigang Chen [a,1], Jingkai Li [a,1], Wei Wang [a], Xiaoxian Guo [b], Yongquan Li [a], Xuming Mao [a], Xinyu Chen [c], Wenjun Guan [a,*]

[a] Zhejiang University, College of Life Sciences, Hangzhou, China
[b] Cornell University, Division of Nutritional Sciences, Ithaca, NY, USA
[c] Zhejiang Hospital, Hangzhou, China

ARTICLE INFO

Article history:
Received 1 April 2013
Received in revised form 19 November 2013
Accepted 4 December 2013
Available online 12 December 2013

Keywords:
ATP-binding cassette transporter
Drug susceptibility
Transmembrane helix
ATPase activity
Yeast

ABSTRACT

As a mammalian p-glycoprotein homolog, Pdr5p is a major ATP-binding cassette transporter for cellular detoxification in the yeast *Saccharomyces cerevisiae*. In this study, two novel loss-of-function mutations located adjacent to the ends of the predicted transmembrane helices of Pdr5p were identified. C793F and S1230L mutations considerably impaired the transport activity of Pdr5p without affecting the ATPase activity and the expression level of the protein. Our results demonstrate that the size of residue 793 and the hydrophobicity of residue 1230 are important for Pdr5p efflux function. It reveals that amino acid residues located near the end of transmembrane helix play an important role in drug efflux of Pdr5p. Molecular docking results further suggest that these two single mutations might have disturbed interactions between the drugs and Pdr5p, preventing the drugs from approaching the intracellular or extracellular portal and subsequently from being exported by Pdr5p.

1. Introduction

Efflux of xenobiotics by ATP-binding cassette (ABC) transporters is a major mechanism employed by various cells to survive in toxic environment [1]. As the best-studied and most abundant ABC transporter in *Saccharomyces cerevisiae*, Pdr5p mediates cellular detoxification and multidrug resistance (MDR) [2,3]. The predicted topological structure of Pdr5p shows that it contains two nucleotide binding domains (NBDs) and two transmembrane domains (TMDs) which harbor twelve transmembrane helices (TMHs), six extracellular loops (ECLs) and four intracellular loops (ICLs) [4,5].

Pdr5p shares similar secondary topological structure with other homologous ABC transporters and is presumed to extrude substrates by continuous switching between inward-facing and outward-facing conformations, which are believed to have different affinities towards the transported substrates [2]. Although TMDs of ABC transporter are not conserved in length or sequence, it is well accepted that TMDs are essential for substrate recognition, binding and translocation, and the amino acid residues within TMHs might play the important roles [6–9].

To clarify the mechanisms of how Pdr5p recognizes and extrudes a wide variety of compounds out of the cells, numerous mutants had been generated by random or site-directed mutagenesis [10–16]. Despite the effort, the structure–function mechanism of Pdr5p still remains unclear [17–19]. A number of single-point mutations within the TMDs had reportedly altered drug specificity or impaired drug-efflux efficiency of Pdr5p [10–12,14,20]. Some of them were thought to have altered how substrates gain access to or release from the substrate-binding pocket through the portal while the others were shown to be defective in the cross-talk between TMDs and NBDs during the catalytic cycle of Pdr5p.

In this study, we identified two novel loss-of-function mutations C793F and S1230L within the TMDs of Pdr5p. To investigate the potential loss-of-function mechanism, C793 and S1230 were individually substituted with various amino acids and drug susceptibility of each mutant was evaluated. Furthermore, we used a recent published 3D model of Pdr5p to perform an independent docking study, shedding more light into the structure–function relationship of Pdr5p.

2. Materials and methods

2.1. Strains, plasmids and media

The strains and plasmids used in this study are listed in Table 1. *S. cerevisiae* BY4741 cells were grown in synthetic complete medium

* Corresponding author. Tel./fax: +86 571 88208 569.
E-mail address: guanwj@zju.edu.cn (W. Guan).
[1] These authors contributed equally to this work.

0005-2736/$ – see front matter © 2013 Elsevier B.V. All rights reserved.
http://dx.doi.org/10.1016/j.bbamem.2013.12.002

Table 1
Strains and plasmids used in this study.

Strains or plasmids	Relevant characteristics	References
S. cerevisiae BY4741	MATa his3 leu2 metl5 ura3	Yeast Knock-out (YKO) deletion collection
E. coli DH5a	*supE44, AlacU169 (q80lacZAM15), hsdR17, recA1, endA1, gyrA96,thi-1, relA1*	
BY4741Apdr5::YEplac195 (DEL)	*MATa his3 leu2 met 15 ura3 pdr5::loxP*	[18]
BY4741Apdr5::YEplac195-BPDR5 (WT)	*MATa his3 leu2 met 15 ura3 pdr5::loxP PDR5*	[18]
BY4741Apdr5::YEplac195-BPDR5-C793M	*MATa his3 leu2 met 15 ura3 pdr5::loxP PDR5-C793M*	This study
BY4741Apdr5::YEplac195-BPDR5-C793S	*MATa his3 leu2 met 15 ura3 pdr5::loxP PDR5-C793S*	This study
BY4741Apdr5::YEplac195-BPDR5-C793F	*MATa his3 leu2 met 15 ura3 pdr5::loxP PDR5-C793F*	This study
BY4741Apdr5::YEplac195-BPDR5-C793Y	*MATa his3 leu2 met 15 ura3 pdr5::loxP PDR5-C793Y*	This study
BY4741Apdr5::YEplac195-BPDR5-S1230F	*MATa his3 leu2 met 15 ura3 pdr5::loxP PDR5-S1230F*	This study
BY4741Apdr5::YEplac195-BPDR5-S1230Y	*MATa his3 leu2 met 15 ura3 pdr5::loxP PDR5-S1230Y*	This study
BY4741Apdr5::YEplac195-BPDR5-S1230A	*MATa his3 leu2 met 15 ura3 pdr5::loxP PDR5-S1230A*	This study
BY4741Apdr5::YEplac195-BPDR5-S1230N	*MATa his3 leu2 met 15 ura3 pdr5::loxP PDR5-S1230N*	This study
BY4741Apdr5::YEplac195-BPDR5-S1230L	*MATa his3 leu2 met 15 ura3 pdr5::loxP PDR5-S1230L*	This study
BY4741Apdr5::YEplac195-BPDR5-S1230P	*MATa his3 leu2 met 15 ura3 pdr5::loxP PDR5-S1230P*	This study
BY4741Apdr5::YEplac195-BPDR5-E794K	*MATa his3 leu2 met 15 ura3 pdr5::loxP PDR5-E794K*	This study
BY4741Apdr5::YEplac195-BPDR5-E794Q	*MATa his3 leu2 met 15 ura3 pdr5::loxP PDR5-E794K*	This study
Plasmids		
YEplac195		ATCC 87589
YEplac195-BPDR5		[18]
YEplac195-BPDR5-C793M		This study
YEplac195-BPDR5-C793S		This study
YEplac195-BPDR5-C793F		This study
YEp\ac195-BPDR5-C793Y		This study
YEp\ac195-BPDR5-S1230F		This study
YEp\ac195-BPDR5-S1230Y		This study
YEp\ac195-BPDR5-S1230A		This study
YEp\ac195-BPDR5-S1230N		This study
YEp\ac\95-BPDR5-S1230L		This study
YEp\ac\95-BPDR5-C793FS1230L		This study
YEp\ac\95-BPDR5-E794Q		This study
YEp\ac\95-BPDR5-E794K		This study

lacking uracil (SD-ura). *Escherichia coli* strain DH5α was served as the host strain for all plasmid constructions and grown in LB medium with 50 μg/ml ampicillin.

2.2. Chemicals

Cycloheximide (CYH), rhodamine 6G (R6G) and FK-506 monohydrate were dissolved in ethanol, whereas the 2,3,5-Triphenyltetrazolium chloride (TTC) and fluconazole (FLC) stock solutions were prepared with sterile water. All reagents above were purchased from Sigma-Aldrich.

2.3. Random and site-directed mutagenesis

PCR-targeted random mutagenesis was performed as previously described [21] and functional impaired mutants were screened using SD-ura agar plate containing 20 μM FLC. The detailed procedure of random mutagenesis and mutant screening is described in Supplementary materials.

Site-directed mutagenesis was performed using QuickChange kit (Stratagene) and YEplac195-*BPDR5* was used as the template. The resulting mutants were confirmed by DNA sequencing. The primers used in sequencing and mutagenesis are listed in Table S1 (Supplementary materials). All the mutational YEplac195-*PDR5* series were transformed into *pdr5*-null mutant strain following LiAc/SS carrier DNA/PEG method as previously described [22].

2.4. Preparation of purified membrane vesicles and immunoblotting

The plasma membrane (PM) vesicles were purified as previously described [13,16]. The concentration of membrane protein in the vesicles was determined by micro-Bradford assay (Bio-Rad Laboratories). Protein profiles (20 μg/lane) were examined by 7% sodium dodecyl sulfate-polyacrylamide gel electrophoresis (SDS-PAGE) followed by Coomassie Blue staining. Western blotting was carried out with a Pdr5-specific antibody yN-18 and a Pma1-specific antibody yN-20 (Santa Cruz Biotechnology, Santa Cruz, CA). yN-18 and yN-20 were 600- and 1000-fold diluted in Tris-Buffered Saline Tween-20 (TBST), respectively. HRP labeled donkey anti-goat polyclonal antibody (Beyotime Biotech, China) was diluted 1:3000 in TBST. Proteins were visualized by ECL chemiluminescence detection system (Beyotime Biotech, China) according to the manufacturer's instructions.

2.5. Drug resistance assays

Fresh yeast cells of BY4741Δ*pdr5*::YEplac195-*BPDR5* (WT), BY4741 Δ*pdr5*::YEplac195 (*pdr5*Δ) and BY4741Δ*pdr5*::YEplac195-*PDR5** harboring various *PDR5* mutant genes were inoculated to 5 ml SD-ura media and grown overnight at 30 °C. Then the cell suspensions were diluted to OD_{600} of 0.1 with sterile SD-ura medium. 6 μl of 5-fold serial dilutions was spotted on SD-ura agar plates containing FLC, CYH or TTC. The plates were incubated at 30 °C for 48 h before scanning. Equal amounts of cells (final $OD_{600} = 0.1$) were cultured in 200 μl SD-ura media containing FLC, CYH or TTC and the final OD_{600} were measured by spectrophotometry after incubation at 30 °C with shaking at 250 rpm for 24 h. The mean relative growth rate was determined by OD_{600} ratio of the cell samples cultured in SD-ura media with/without the drugs.

2.6. Determining the inhibitory concentration 50 (IC_{50}) of a drug in liquid culture

Fresh yeast cells were inoculated to 5 ml SD-ura medium and grown overnight at 30 °C. Then the cultures were diluted to OD_{600} of 0.1 with sterile SD-ura medium. 200 μl of above cultures were transferred to a

96-well plate containing the tested drug at the indicated concentrations. The 96-well plate was then incubated for 24 h at 30 °C with shaking (250 rpm). The percent inhibition was determined by the ratio of OD_{600} of the culture grown in the presence or absence of a drug at various concentrations and the test was repeated for three separate inoculations unless indicated otherwise. Data points were plotted using GraphPad Prism 5 software and the IC_{50} values were determined from the graph.

2.7. Rhodamine 6G (R6G) transport assay

Transport of R6G was determined as previously described [11]. Yeast cells were grown in SC-ura media to an OD_{600} of 2. To measure dye efflux, cells were washed with 50 mM HEPES buffer (pH7) twice and resuspended in 500 μl 50 mM HEPES buffer containing 5 μM or 50 μM R6G, followed by a 60 min incubation at 30 °C. After a centrifugation for 15 min at 12,000 *g* and 30 °C, cells were resuspended in pre-warmed 50 mM HEPES buffer containing 2.5 mM glucose to initiate R6G efflux. After incubation for 40 min at 30 °C, R6G efflux was stopped by 5 min incubation on ice. The cells were washed with pre-cooled 50 mM HEPES buffer once and resuspended in 500 μl HEPES buffer. Intracellular rhodamine fluorescence was analyzed with Beckman Coulter (Cytomics FC500MCL) using CXP software.

2.8. ATPase activity assay

Pdr5p-associated ATPase activities of the purified PM were measured as previously described [13,16,23]. Purified PM vesicles (0.5 μg protein per well) were incubated with 5 mM ATP in 25 μl 150 mM MOPS Buffer (pH7.5) containing 50 mM KNO_3, 10 mM NaN_3, 0.2 mM $(NH_4)_2MoO_4$, 5 mM $MgCl_2$ and 10 μM sodium orthovanadate (Na_2VO_4) for 20 min at 30 °C. The reactions were terminated by the addition of 175 μl ice-cold 40 mM H_2SO_4. The amount of released inorganic phosphate was determined by a colorimetric assay, using Na_2HPO_4 as standard [24]. The absorbance data were collected by using a Power Wave XS microplate spectrophotometer equipped with Gen5 software (BioTek).

2.9. Molecular docking

The structures of CYH, FLC, TTC and R6G were downloaded from PubChem with CID 6197, 3365, 9283 and 13806, respectively. LigPrep program in Maestro (v9.0) was used to optimize the structures of four compounds with the default parameters. The inward-facing structure of Pdr5p [4] based on mouse P-glycoprotein template [19] was prepared as follows. First, hydrogen atoms were added. Then, the resultant structure was energy-minimized for 1000 steps using the OPLS_2005 force field [25] with all the non-hydrogen atoms constrained to their original positions. The Glide program (v4.0) [26,27] was used to predict the binding conformation between a compound and the inward-facing structure of Pdr5p. First, the inward-facing structure of Pdr5p was prepared using the protein preparation wizard in Maestro, and all the parameters were set to default except that the minimization was for hydrogens only. Then the two receptor grids were generated as follows: C793 and S1230 were defined as the centroid of Enclosing Box. The size limit of the box was set to 20 Å. These two Enclosing Boxes were defined as two binding pockets around C793 and S1230. The atoms in C793 and E794 that could participate in hydrogen bonding were picked in the constraints section for the grid generation of the binding pocket around C793, and the atoms in S1230 that could participate in hydrogen bonding were picked in the constraints section for the grid generation of the binding pocket around S1230. Other parameters used in receptor grid generation were set to their defaults. Finally, each of the three compounds were docked to the two binding pockets using the standard precision mode. During docking, 500,000 poses per ligand for the initial phase of docking were kept and 40,000 poses per ligand for energy minimization were kept. The constraints for hydrogen bonds were set to match at least once, and test constrain satisfaction was applied only after docking. For each compound–binding pocket pair, Glide reported 20 best binding conformations in both precision modes.

3. Results

3.1. Isolation of loss-of-function Pdr5p mutants

Previous studies had identified several loss-of-function mutants conferred by single amino acid change within TMHs or NBDs of Pdr5p [11–16]. To identify more novel mutations important for Pdr5p function, Pdr5p variants were created by random mutagenesis. After screening, two novel mutants (C793F and S1230L) exhibiting FLC hypersensitivity similar to *pdr5*Δ cells were identified. As shown in Fig. 1, the mutants are hypersensitive to FLC both on agar plates and in liquid media. The S1230L mutant was more sensitive to FLC (IC_{50} of ~15 μM) than the C793F mutant (IC_{50} of ~65 μM) corresponding to a ~4 fold difference in sensitivity, whereas the WT strain and the *pdr5*Δ strain had FLC IC_{50} of ~160.1 μM and ~4.9 μM, respectively (Table S2).

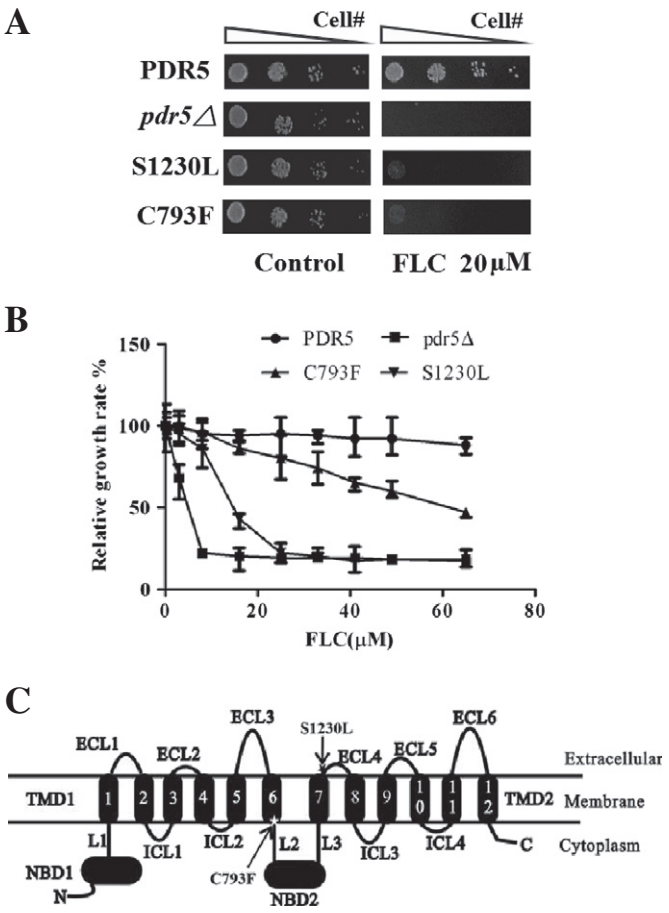

Fig. 1. Growth of the C793F and S1230L mutants was inhibited by FLC. (A) The susceptibility of the C793F and S1230L mutants to FLC was compared in spot assay. Spots were prepared with 1:5 serial dilutions of the cell suspensions (OD_{600} = 0.1). The drug plates were incubated at 30 °C for 48 h. (B) The susceptibility of the C793F and S1230L mutants to FLC was also compared in liquid culture. OD_{600} was measured after 24 h incubation. Each point is the average of three samples. (C) Schematic representation based on a topology prediction [4] of Pdr5p, showing the positions of C793 and S1230.

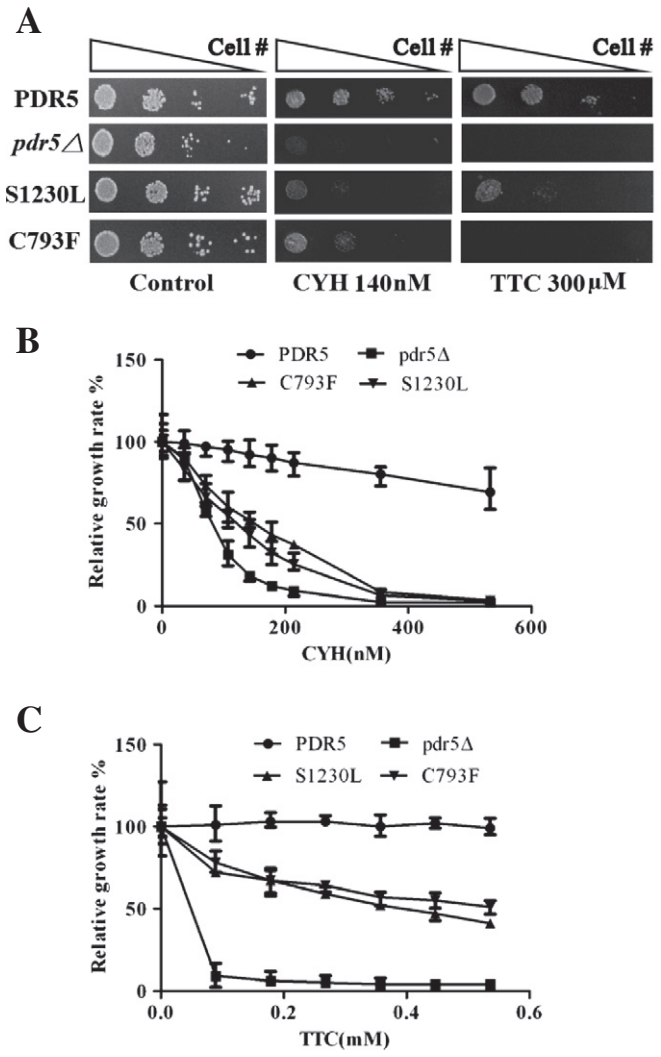

Fig. 2. Growth of the C793F and S1230L mutants was also inhibited by CYH and TTC. (A) The susceptibility of the C793F and S1230L mutants to CYH and TTC was compared in spot assay. Spots were prepared with 1:5 serial dilutions of the cell suspensions (OD_{600} = 0.1). The drug plates were incubated at 30 °C for 48 h. The susceptibility of the C793F and S1230L mutants to CYH (B) and TTC (C) was also compared in liquid culture. OD_{600} was measured after 24 h incubation. Error bars represent the standard deviations of triplicate experiments.

3.2. Drug resistance phenotypes of C793F and S1230L mutants

The Pdr5p substrates FLC, CYH, R6G and TTC [12] are different in size, hydrophobicity, chemical composition and surface charge density (Table S3). To investigate whether C793F and S1230L mutants cause a global reduction in drug efflux, we studied the drug susceptibility of the mutants towards CYH and TTC and their intracellular accumulation of R6G.

As shown in Fig. 2A, both mutants are hypersensitive to CYH and TTC on the agar plates. Growth of cells harboring the C793F or S1230L mutant was clearly reduced in the liquid media containing CYH (Fig. 2B) or TTC (Fig. 2C) at the indicated concentrations. IC_{50}s were about 156 nM (CYH) and 535 μM (TTC) for C793F cells, and about 124 nM (CYH) and 357 μM (TTC) for S1230L cells (Table S2). These values were higher than those of the *pdr5Δ* cells, but much lower than those of the WT cells, demonstrating markedly impaired efflux of CYH and TTC in these mutants. There was no evidence of Pdr5p drug specificity change caused by C793F or S1230L mutation.

The intracellular accumulation of R6G was determined by flow cytometry analysis of dye-preloaded cells expressing Pdr5 mutants (Fig. 3). Yeast cells expressing the C793F or S1230L mutant exhibited

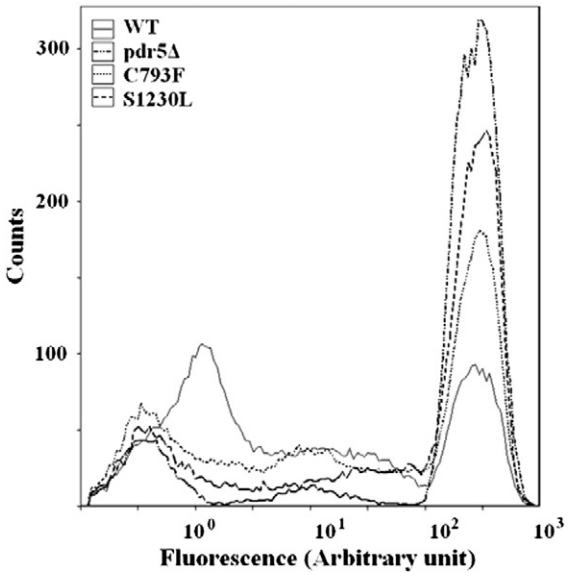

Fig. 3. R6G transport was impaired in the S1230L and C793F mutants. The data were shown from the experiment in which 50 μM R6G was preloaded for 60 min into cells at 30 °C in buffer lacking glucose prior to efflux in HEPES buffer containing 2.5 mM glucose for 40 min. Plots were constructed from counts of 50,000 cells per sample.

an increased intracellular fluorescence intensity compared with that of WT Pdr5p, demonstrating their reduced R6G efflux capacity. To rule out other possibilities leading to drug hypersensitivity of the mutants, we then isolated PM fractions to study the expression level, subcellular localization and Pdr5p-specific ATPase activity of the mutants. Our results showed that the expression levels of C793F and S1230L mutants were nearly identical to that of wild-type Pdr5p (Fig. 4A) and no obvious reduction of ATPase activity was observed in these mutants (Fig. 4B). It indicates that neither C793F nor S1230L mutation affects ATPase activity, protein localization, or expression level of Pdr5p.

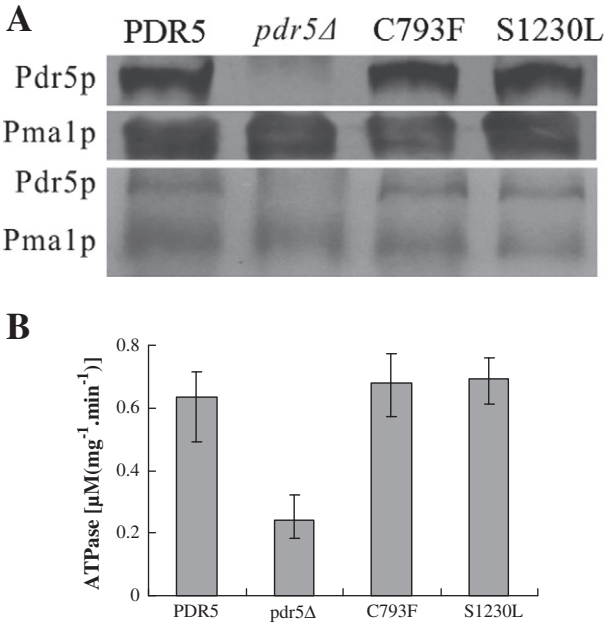

Fig. 4. Pdr5p expression level, localization and ATPase activity were not affected by the C793F and S1230 mutations. (A) Expression levels of mutant Pdr5 proteins. Membrane protein was isolated as described in Materials and methods and subjected to SDS-PAGE followed by Coomassie Blue staining (lower panel) and anti-Pdr5 western blotting (upper panel). (B) Pdr5p-specific ATPase activities of the C793F and S1230L mutants. The values represent at least three independent experiments carried out with three different plasma membrane vesicle preparations of each strain.

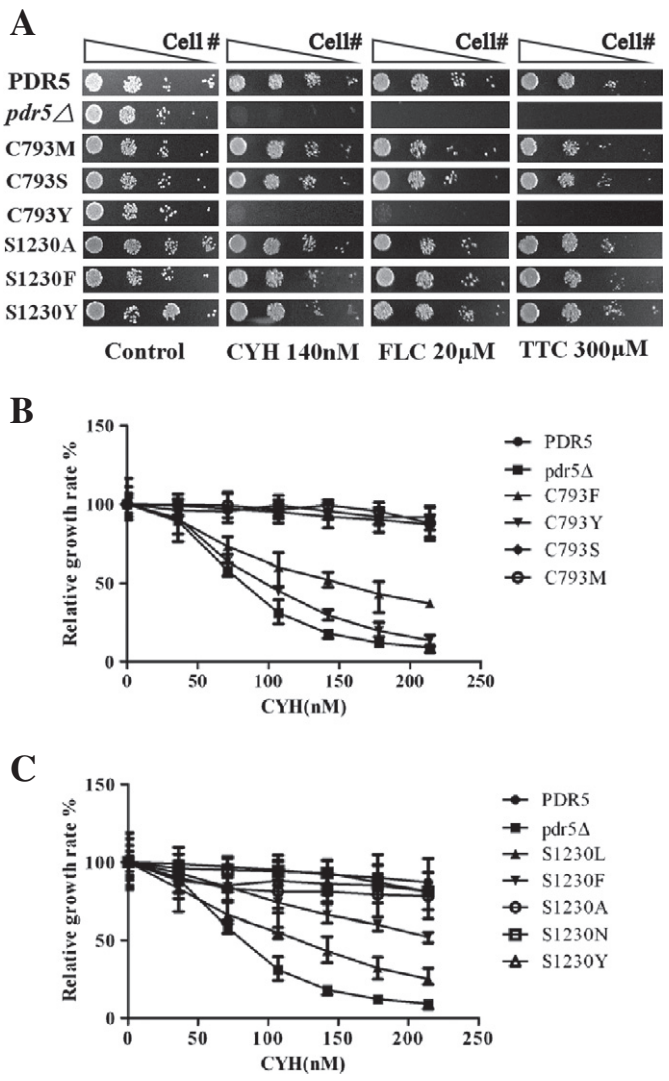

Fig. 5. Mutational analysis of Pdr5. (A) Spot assay on SD-ura agar plates containing CYH, FLC, TTC, respectively. Liquid culture assay of drug resistance of C793 (B) and S1230 (C) mutants in SD-ura liquid medium containing CYH. Error bars represent the standard deviations of triplicate experiments.

In addition, we also examined the inhibitory effect of immunosuppressant FK506, a known inhibitor/substrate of Pdr5p [20], on cells harboring S1230L or C793F mutation. As shown in Fig. S3, *pdr5Δ* cells were unable to grow in the presence of 2 μg/ml FLC, whereas cells harboring WT Pdr5, S1230L or C793F mutant exhibited no obvious growth inhibition. Simultaneous exposure of WT cells and C793F mutant to both FLC and FK506 totally abolished growth, demonstrating inhibition of FLC transport by FK506. However, the S1230L mutant exhibited a decreased FK506 inhibition, suggesting that S1230L mutation might have disturbed FK506–Pdr5 interaction.

Table 2
Drug susceptibility ranking of *S. cerevisiae* cells expressing the wild type and mutant variant of Pdr5p.

Drug (conc.)	Residue position	Drug susceptibility
CYH (178 nM)	C793	Y > F > M, S, C
FLC (49 μM)	C793	Y > F > M > S, C
TTC (0.5 mM)	C793	Y > F, M > S, C
CYH (178 nM)	S1230	L > F > Y, A, N > S
FLC (49 μM)	S1230	L > F > N > Y, A, S
TTC (0.5 mM)	S1230	L > F > Y > A > N > S

3.3. Residue substitution study at positions 793 and 1230

To understand how substitution of C793F or S1230L impairs Pdr5p-mediated drug efflux, C793S, C793M, C793Y, S1230A, S1230Y, S1230N and S1230F mutants were generated by site-directed mutagenesis to compare their drug susceptibility. As shown in Fig. 5, besides C793F and S1230L, the C793Y mutant was also hypersensitive to all drugs tested on the agar plates (Fig. 5A) and to CHY in liquid media (Fig. 5B). The drug resistance assays showed that the C793Y mutant was more sensitive to the drugs tested than the C793F mutant. As shown in Table S2, the C793Y mutant exhibited lower IC_{50}s than the C793F mutant in the present of the drugs. The expression level, subcellular localization and ATPase activity of the C793Y mutant were similar to that of wild-type Pdr5p (Fig. S1).

Table 2 shows the drug susceptibility ranking of all the Pdr5 mutants mentioned above towards the chemicals tested at a selected concentration. Generally, at position 793, substituting Cys (volume: 108.5 $Å^3$) with a bulky residue, Met (162. 9 $Å^3$), Phe (189.9 $Å^3$) or Tyr (193.6 $Å^3$) [28] increasingly impaired Pdr5p-mediated substrate efflux capacity whereas substituting with the small Ser (89 $Å^3$) did not show obvious effect (Fig. 5B). Similar to Cys, Tyr is a polar residue, but the C793Y mutant is more sensitive towards the drugs than the C793F mutant, indicating that residue hydrophobicity is not important at position 793. At position 1230, according to the estimated contribution of the hydrophobic effect to the burial of amino acid residue calculated by P. Andrew Karplus [29], residue hydrophobicity is systematically increased by replacing the serine residue (1.4 kcal/mol) with more hydrophobic Tyr (2.81 kcal/mol), Phe (3.46 kcal/mol) or Leu (4.1 kcal/mol), respectively. As shown in Fig. 5C, the sensitivity of the S1230 mutants towards CYH indeed increased with the rise of residue hydrophobicity. However, residue size is not important at position 1230, because substitution of Ser (89 $Å^3$) with Tyr (193.6 $Å^3$) did not change the drug resistance pattern of Pdr5p. These results indicate that size of the residue at position 793 and hydrophobicity of the residue at position 1230 are important for drug efflux.

3.4. Double mutant analysis

According to a recent published 3D model [4], TMH6 and TMH7 of Pdr5p comprise approximately amino acid residues 772–795 and 1203–1228, respectively. S1230 is located at the extracellular end of the predicted TMH7, whereas C793 is located at the intracellular end of the predicted TMH6 (Fig. 1C). Our mutant analysis revealed that both the C793F and S1230L mutants conferred drug hypersensitivity compared with WT Pdr5p, but they probably rely on different mechanisms. To further investigate the role of the two residues, we constructed the C793F/S1230L double mutant.

Like the C793F and S1230L mutants, the expression level, subcellular localization or ATPase activity of the double mutant was similar to that of WT Pdr5p (Fig. 6A, B). As shown in Fig. 6C, the double mutant protein exhibited a markedly decreased CYH resistance, demonstrating that there is additive effect of the two mutations. IC_{50}s were about 84.1 nM (CYH), 6.9 μM (FLC) and 128 μM (TTC) for C793F/S1230L cells (Table S2). These values were similar to those of the *pdr5Δ* cells.

In addition, similar to WT Pdr5p, the intracellular accumulation of R6G in the C793F/S1230L mutant showed no obvious change both at low and high R6G concentrations (5 μM and 50 μM) in the presence of CYH (Table 3), TTC and FLC (Table S4), indicating that the drugs tested could not compete with R6G efflux in the cells expressing S1230L, C793F or the double mutant. It revealed that neither C793 nor S1230 belongs to the common binding sites for R6G and the drugs tested.

3.5. Docking of the drugs to Pdr5p

In order to evaluate the interactions between Pdr5p and the four drugs, we performed docking experiments on Pdr5p. Our docking

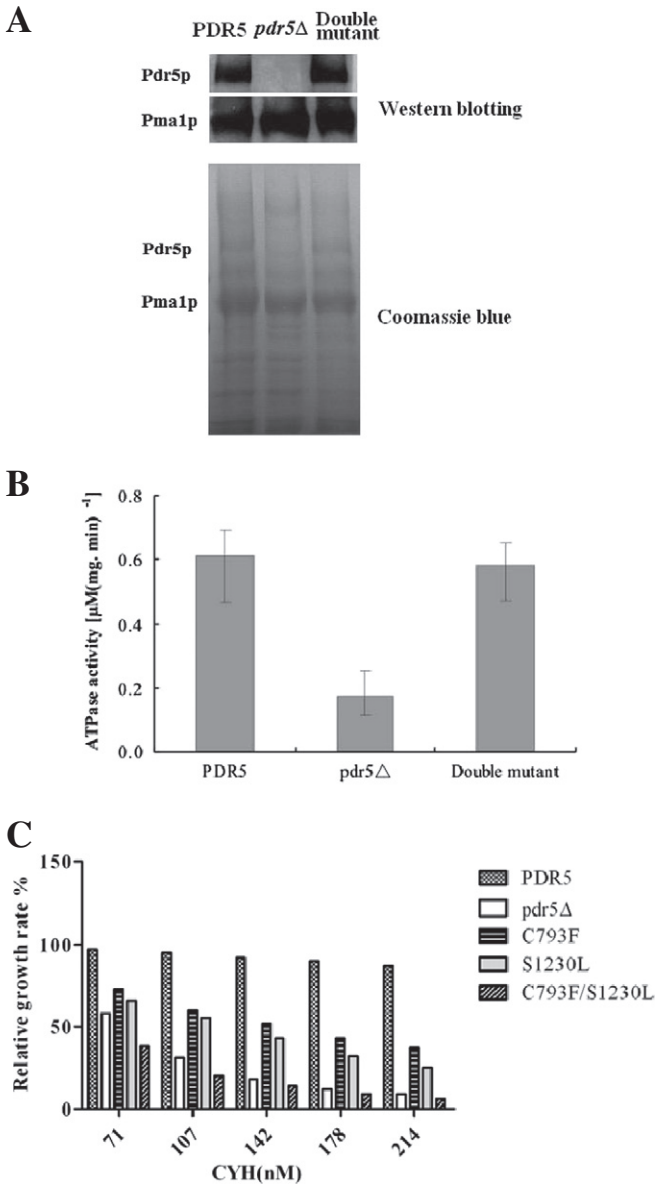

Fig. 6. The C793F/S1230L double mutant exhibited a markedly decreased CYH resistance. (A) Expression levels of mutant Pdr5 protein. Protein was isolated as described in Materials and methods and subjected to SDS-PAGE followed by Coomassie Blue staining (lower panel) and anti-Pdr5 western blotting (upper panel). (B) Pdr5p-specific ATPase activity of the C793F/S1230L double mutant. The values represent at least three independent experiments carried out with three different plasma membrane vesicle preparations of each strain. (C) Liquid culture assay of CYH resistance of the double mutant. Each point is the average of three samples.

analysis indicates that CYH, FLC, R6G and TTC were all able to interact with the modeled inward-facing conformation of Pdr5p with satisfactory fitness scores.

Docking of the drugs to modeled Pdr5p showed that CYH, FLC and R6G could be docked into the binding pocket containing C793 and E794 in the inward-facing conformation of Pdr5p (Fig. 7B–D). Though there is no direct interaction between the C793 and the compounds, the E794 does form hydrogen bonds with CYH, FLC and R6G except TTC. C793 is a medium sized residue and its mutation may interfere with the hydrogen bond interactions between E794 and the substrates. These hydrogen bonds are in locations that may help stabilize the conformations of Pdr5p substrates for passing through the transport channel efficiently.

According to the docking experiments, S1230 directly formed hydrogen bonds with all the compounds except TTC (Fig. 7F–H). Because S1230 is close to the extracellular end of the predicted TMH7, the mutation at this residue may prevent the drugs from approaching the extracellular portal and subsequently their release from Pdr5p by disturbing the hydrogen bond formation of the drugs with S1230.

Our docking analysis found no hydrogen bond interaction between TTC and the two residues above (Fig. 7E, I). In fact, TTC has three hydrogen donors and no hydrogen acceptor, whereas the other three compounds have at least 6 donors/acceptors (Table S3). Three benzene rings around the central tetrazolium make it hard for external hydrogen acceptors to access these donors. Lacking hydrogen bonds between TTC and Pdr5p implied an inferior fitting between TTC and the Pdr5p channel. As shown in Table S5, TTC exhibited quite strong van der Waals interactions with the drug-binding pockets. The results indicate the structural basis for the sensitivity of the mutants to TTC.

4. Discussion

To understand the structure–function relationship of Pdr5p, we used PCR-targeted random mutagenesis to generate Pdr5 mutants and identified two novel single mutations that led to significant reduction in Pdr5p-mediated FLC resistance. The drug-susceptibility assay confirmed that both the C793F and S1230L mutants could not effectively extrude four physically and chemically diverse drugs tested. It is noteworthy that both mutants retained Pdr5p-specific ATPase activity. To explore the loss-of-function mechanisms of these mutations, Cys793 and Ser1230 were substituted with a series of amino acids different in size or hydrophobicity. Our results demonstrate that the relatively small size of residue 793 and the hydrophobicity of residue 1230 are important for Pdr5p function.

Residue C793 is located adjacent to the intracellular end of the predicted TMH6 of Pdr5p, near the predicted intracellular boundary of the substrate-binding pocket. Although C793 is not conserved according to sequence alignment result, high conservation of its neighboring residue E794 in fungal ABC transporter gene family suggests that certain property of the residue at position 793 may be of some functional importance (Fig. S1). Our site-directed mutagenesis result confirmed that the E794Q and E794K mutants exhibited markedly impaired efflux of R6G, demonstrating that the negatively charged residue at position 794 is very important for Pdr5p function (Fig. S4). Interestingly, such phenomenon had also been observed in our previous work on the A1352M mutant [16]. Like E794, a highly conserved E1353, the

Table 3
The intracellular R6G accumulation of Pdr5 mutants in the presence of cycloheximide.

	Relative % of intracellular R6G							
	R6G 5 μM				R6G 50 μM			
	CYH 0 μM	CYH 0.18 μM	CYH 0.53 μM	CYH 0.89 μM	CYH 0 μM	CYH 1.8 μM	CYH 5.3 μM	CYH 8.9 μM
PDR5	11.5	17.8	14.1	14.9	17.0	15.2	15.5	15.3
*pdr5*Δ	76.5	67.8	56.9	65.4	81.9	90.7	91.9	90.6
C793F	29.2	26.3	26	25.6	53	57.2	54.5	53.3
S1230L	65.6	61.8	60.2	57.7	73.1	75.9	75.1	75.5
C793F S1230L	64.3	59.8	56.7	62.8	89.3	89	88.5	89.6

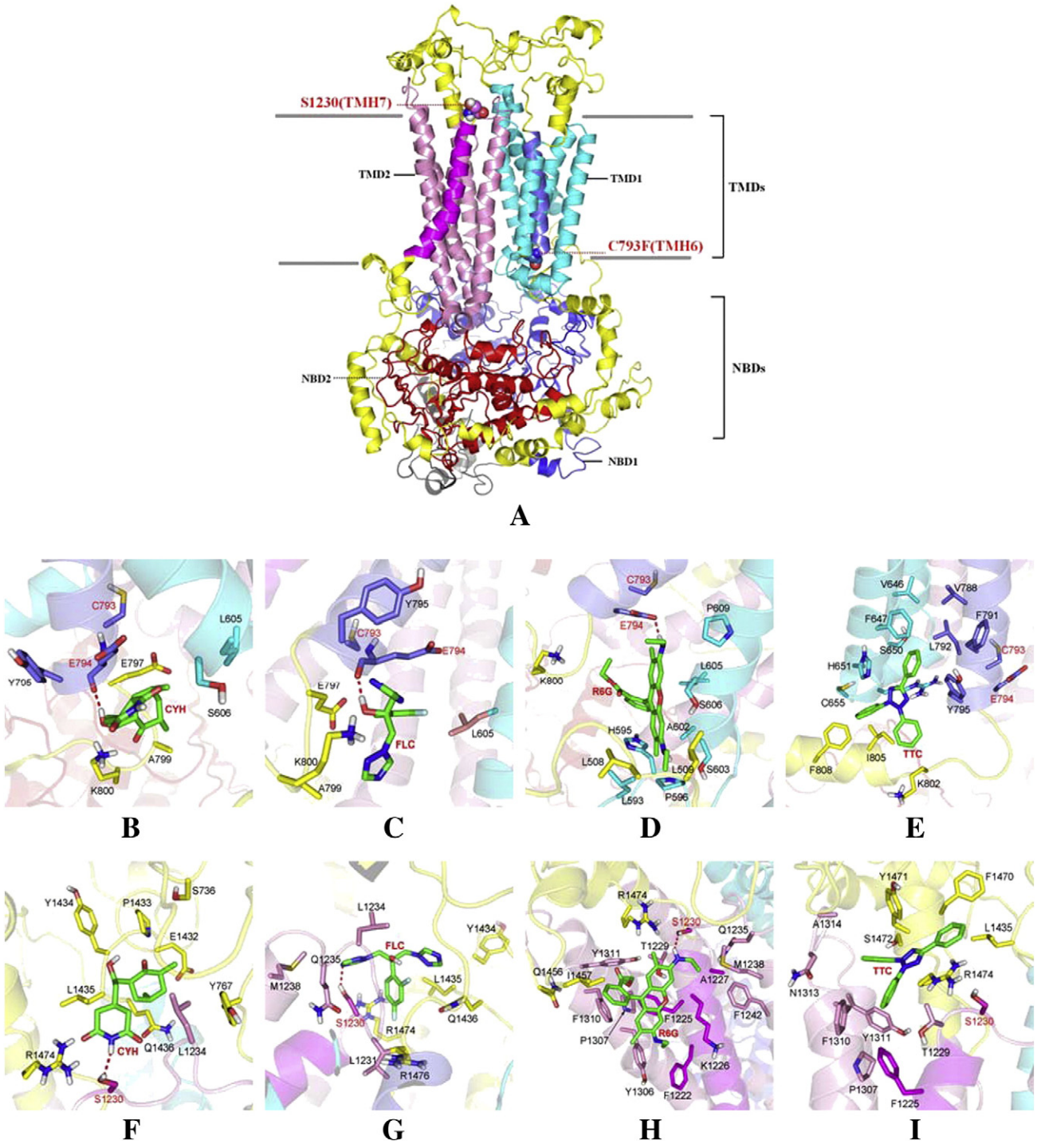

Fig. 7. Substrate docking in Pdr5p. (A) Stereoscopic view of the Pdr5p model based on mouse P-glycoprotein template. The two modeled TMDs, colored powder-blue and pink, are embedded in a membrane bilayer. Underneath the TMDs are the NBDs (NBD1 in blue, NBD2 in red). The extracellular loops sit above the TMDs (yellow). Residues C793 and S1230 are marked with red dashed line [4]. Predicted binding models of CYH (B), FLC (C), R6G (D) and TTC (E) to Pdr5p around C793. Predicted binding models of CYH (F), FLC (G), R6G (H) and TTC (I) to Pdr5p around S1230. Hydrogen bonds are depicted with dashed lines.

neighboring residue of A1352, is also located at the intracellular interface of the substrate-binding pocket. Replacement of A1352 with bulky methionine severely disturbed the transport activity of Pdr5p. These results reveal that the bulky residue substitution at the neighboring residues of E794 or E1353 impairs the efflux capability of Pdr5p without disturbing its ATPase activity, implying that these conserved, charged residues located at the membrane–cytosol interface of TMHs are important for the binding/transport of efflux pump substrates. An increased residue size at position 793 may block Glu794 from forming hydrogen bonds or van der Waals interactions with the drugs, resulting in impaired efflux capability of Pdr5p. According to the recent topological structure model reported, Pdr5p contains over 13 charged residues predicted to reside at the membrane–cytosol interface of TMHs, and most of them are highly conserved [4]. Thorough investigation on these conserved, charged residues will provide more insight into the function–structure relationship of Pdr5p.

In contrast to C793, S1230 is proximal to the extracellular end of the predicted TMH7. S1230 is highly conserved among fungal Pdr proteins (Fig. S1), indicating that it may play a very important functional role in Pdr5p-mediate drug export. It was found that substituting the polar serine with a highly hydrophobic leucine (S1230L) indeed resulted in severe impairment on drug efflux. Although four chemicals tested in this study have different scale of hydrophobicity (determined as logP), the S1230L mutant exhibited no obvious substrate specificity change. Replacing Ser1230 with bulky residues had no obvious effect on the efflux capacity of Pdr5p, implying that S1230 is probably not located at a critical location that may prevent substrates from passing through the transport channel.

Furthermore, the molecular docking results suggested that these two single mutations might have disturbed hydrogen bond formation and van der Waals interactions of Pdr5p with the tested drugs, preventing the drugs from approaching the intracellular or extracellular portal, and subsequently impaired the efflux efficiency of Pdr5p.

In summary, our new observation that both the C793F and S1230L mutants considerably impaired the transport activity of Pdr5p without affecting the ATPase activity, localization and the expression level of the protein paves a way for future investigations on the role of TMH-interface residues in substrate transport.

Acknowledgements

This work was supported by the National Natural Science Foundation of China (No. 31170032) and National High Technology Research and Development Program of China (No. 2011AA040406). We thank Dr. Di Xia and Dr. Robert M Rutledge from NIH for sharing the atomic model of Pdr5p with us. We also thank Dr. Xin Chen, Dr. Sheng Ye for paper discussion and Dr. Yingchun Liu for spatial volume calculation of the chemical compounds.

Appendix A. Supplementary data

Supplementary data to this article can be found online at http://dx.doi.org/10.1016/j.bbamem.2013.12.002.

References

[1] B.C. Monk, A. Goffeau, Outwitting multidrug resistance to antifungals, Science 321 (2008) 367–369.
[2] R. Ernst, P. Kueppers, J. Stindt, K. Kuchler, L. Schmitt, Multidrug efflux pumps: substrate selection in ATP-binding cassette multidrug efflux pumps—first come, first served? FEBS J. 277 (2010) 540–549.
[3] B. Rogers, A. Decottignies, M. Kolaczkowski, E. Carvajal, E. Balzi, A. Goffeau, The pleitropic drug ABC transporters from *Saccharomyces cerevisiae*, J. Mol. Microbiol. Biotechnol. 3 (2001) 207–214.
[4] R.M. Rutledge, L. Esser, J. Ma, D. Xia, Toward understanding the mechanism of action of the yeast multidrug resistance transporter Pdr5p: a molecular modeling study, J. Struct. Biol. 173 (2011) 333–344.
[5] M.A. Seeger, H.W. van Veen, Molecular basis of multidrug transport by ABC transporters, Biochim. Biophys. Acta 1794 (2009) 725–737.
[6] R.M. Kennan, L.M. McMurry, S.B. Levy, J.I. Rood, Glutamate residues located within putative transmembrane helices are essential for TetA(P)-mediated tetracycline efflux, J. Bacteriol. 179 (1997) 7011–7015.
[7] Z. Ni, Z. Bikadi, X. Cai, M.F. Rosenberg, Q. Mao, Transmembrane helices 1 and 6 of the human breast cancer resistance protein (BCRP/ABCG2): identification of polar residues important for drug transport, Am. J. Physiol. Cell Physiol. 299 (2010) C1100–C1109.
[8] K. Koike, G. Conseil, E.M. Leslie, R.G. Deeley, S.P. Cole, Identification of proline residues in the core cytoplasmic and transmembrane regions of multidrug resistance protein 1 (MRP1/ABCC1) important for transport function, substrate specificity, and nucleotide interactions, J. Biol. Chem. 279 (2004) 12325–12336.
[9] X.Q. Ren, T. Furukawa, S. Aoki, T. Sumizawa, M. Haraguchi, Y. Nakajima, R. Ikeda, M. Kobayashi, S. Akiyama, A positively charged amino acid proximal to the C-terminus of TM17 of MRP1 is indispensable for GSH-dependent binding of substrates and for transport of LTC4, Biochemistry 41 (2002) 14132–14140.
[10] Z.E. Sauna, S.S. Bohn, R. Rutledge, M.P. Dougherty, S. Cronin, L. May, D. Xia, S.V. Ambudkar, J. Golin, Mutations define cross-talk between the N-terminal nucleotide-binding domain and transmembrane helix-2 of the yeast multidrug transporter Pdr5: possible conservation of a signaling interface for coupling ATP hydrolysis to drug transport, J. Biol. Chem. 283 (2008) 35010–35022.
[11] R. Egner, B.E. Bauer, K. Kuchler, The transmembrane domain 10 of the yeast Pdr5p ABC antifungal efflux pump determines both substrate specificity and inhibitor susceptibility, Mol. Microbiol. 35 (2000) 1255–1263.
[12] A.C. Tutulan-Cunita, M. Mikoshi, M. Mizunuma, D. Hirata, T. Miyakawa, Mutational analysis of the yeast multidrug resistance ABC transporter Pdr5p with altered drug specificity, Genes Cells 10 (2005) 409–420.
[13] R. Ernst, P. Kueppers, C.M. Klein, T. Schwarzmueller, K. Kuchler, L. Schmitt, A mutation of the H-loop selectively affects rhodamine transport by the yeast multidrug ABC transporter Pdr5, Proc. Natl. Acad. Sci. U. S. A. 105 (2008) 5069–5074.
[14] C.P. De Thozee, S. Cronin, A. Goj, J. Golin, M. Ghislain, Subcellular trafficking of the yeast plasma membrane ABC transporter, Pdr5, is impaired by a mutation in the N-terminal nucleotide-binding fold, Mol. Microbiol. 63 (2007) 811–825.
[15] N. Ananthaswamy, R. Rutledge, Z.E. Sauna, S.V. Ambudkar, E. Dine, E. Nelson, D. Xia, J. Golin, The signaling interface of the yeast multidrug transporter Pdr5 adopts a cis conformation, and there are functional overlap and equivalence of the deviant and canonical Q-loop residues, Biochemistry 49 (2010) 4440–4449.
[16] X. Guo, J. Li, T. Wang, Z. Liu, X. Chen, Y. Li, Z. Gu, X. Mao, W. Guan, A mutation in intracellular loop 4 affects the drug-efflux activity of the yeast multidrug resistance ABC transporter Pdr5p, PLoS One 7 (2012) e29520.
[17] R.J. Dawson, K.P. Locher, Structure of the multidrug ABC transporter Sav 1866 from *Staphylococcus aureus* in complex with AMP-PNP, FEBS Lett. 581 (2007) 935–938.
[18] R.J. Dawson, K.P. Locher, Structure of a bacterial multidrug ABC transporter, Nature 443 (2006) 180–185.
[19] S.G. Aller, J. Yu, A. Ward, Y. Weng, S. Chittaboina, R. Zhuo, P.M. Harrell, Y.T. Trinh, Q. Zhang, I.L. Urbatsch, G. Chang, Structure of P-glycoprotein reveals a molecular basis for poly-specific drug binding, Science 323 (2009) 1718–1722.
[20] R. Egner, F.E. Rosenthal, A. Kralli, D. Sanglard, K. Kuchler, Genetic separation of FK506 susceptibility and drug transport in the yeast Pdr5 ATP-binding cassette multidrug resistance transporter, Mol. Biol. Cell 9 (1998) 523–543.
[21] T. Kwan, P. Gros, Mutational analysis of the P-glycoprotein first intracellular loop and flanking transmembrane domains, Biochemistry 37 (1998) 3337–3350.
[22] R.D. Gietz, R.A. Woods, Yeast transformation by the LiAc/SS Carrier DNA/PEG method, Methods Mol. Biol. 313 (2006) 107–120.
[23] J. Golin, Z.N. Kon, C.P. Wu, J. Martello, L. Hanson, S. Supernavage, S.V. Ambudkar, Z.E. Sauna, Complete inhibition of the Pdr5p multidrug efflux pump ATPase activity by its transport substrate clotrimazole suggests that GTP as well as ATP may be used as an energy source, Biochemistry 46 (2007) 13109–13119.
[24] J. Zaitseva, I.B. Holland, L. Schmitt, The role of CAPS buffer in expanding the crystallization space of the nucleotide-binding domain of the ABC transporter haemolysin B from *Escherichia coli*, Acta Crystallogr. D Biol. Crystallogr. 60 (2004) 1076–1084.
[25] G.A. Kaminski, R.A. Friesner, J. Tirado-Rives, W.L. Jorgensen, Evaluation and reparametrization of the OPLS-AA force field for proteins via comparison with accurate quantum chemical calculations on peptides, J. Phys. Chem. B 105 (2001) 6474–6487.
[26] R.A. Friesner, J.L. Banks, R.B. Murphy, T.A. Halgren, J.J. Klicic, D.T. Mainz, M.P. Repasky, E.H. Knoll, M. Shelley, J.K. Perry, D.E. Shaw, P. Francis, P.S. Shenkin, Glide: a new approach for rapid, accurate docking and scoring. 1. Method and assessment of docking accuracy, J. Med. Chem. 47 (2004) 1739–1749.
[27] T.A. Halgren, R.B. Murphy, R.A. Friesner, H.S. Beard, L.L. Frye, W.T. Pollard, J.L. Banks, Glide: a new approach for rapid, accurate docking and scoring. 2. Enrichment factors in database screening, J. Med. Chem. 47 (2004) 1750–1759.
[28] A.A. Zamyatnin, Protein volume in solution, Prog. Biophys. Mol. Biol. 24 (1972) 107–123.
[29] P.A. Karplus, Hydrophobicity regained, Protein Sci. 6 (1997) 1302–1307.